2020 EAGE ANNUAL
82ND CONFERENCE + EXHIBITION
AMSTERDAM | THE NETHERLANDS

Least-squares migration with deep learning based structural constraints

Cheng Cheng*, Yang He, Shuqian Dong, Bin Wang

Summary

Iterative data-domain least-squares migration can overcome acquisition limitations and recover the reflectivity for desired amplitudes and resolutions. However, migration noise due to velocity errors and multiple scattering energy related to strong contrasts in the velocity model can be erroneously enhanced as well. In this complex case, many extra iterations are needed to achieve the final desired image. Regularization can be applied at each least-squares iteration in order to suppress migration artifacts and improve inversion efficiency. However, in sedimentary layers, without proper fault constraints, the regularization cannot preserve the real geological features in the image. In this work, we propose to use convolutional neural networks (CNNs) to automatically detect faults on the migration image first, and then to use the picked fault information as a weighting function for regularization during least-squares migration. With proper training, our 3D predictive model can learn to detect true fault features and avoid erroneous picks of swing noise on the validation dataset. An offshore Brazil field data example in the Santos Basin demonstrates that our final least-squares migration images show enhanced fault structure, minimized migration artifacts, significantly increased image bandwidth and improved illumination after only a few iterations.

Introduction

Many field data examples of data-domain least-squares migration (LSM) have shown that this method can overcome limitations of conventional depth migration, including limited image wavenumber content, biased illumination under complex geology and artifacts due to acquisition limitations (Wang et al., 2013). LSM estimates the reflectivity model by finding the best least-squares fit of the modeled data to the observed data, using gradient-based iterative methods. However, one cannot match all the complex features present in field data with only a linearized Born modeling operator. Without any constraints on the inversion gradient, the noise content will also increase with iterations. This increased noise mostly arises from velocity model error, a wider bandwidth of pre-existing linear noise in the data and back scattered energy due to the presence of strong contrasts in the velocity model (Wang et al., 2016). A successful inversion result requires many more iterations in this case in order to achieve the desired image with high signal-to-noise ratio. It is not efficient for production, especially when applied on high quality large scale multi-client projects which have strict turnaround time. The unacceptably high computational cost for attenuating these kinds of artifacts necessitates a regularization approach that can help to attain a noise-free imaging result more efficiently. Many regularization approaches have been applied to impose constraints on the estimated gradient model, such as shaping regularization and dip filtering in the angle domain to reduce the effect of noise. These approaches work by imposing structure-enhancing filtering operators on the gradient to remove noise while preserving structural information like dipping faults. They essentially calculate semblance along various dips and can detect vertical discontinuities and linear faulting along features in the reflectivity, helping LSM to preserve this kind of information. However, in shallow sedimentary layers where fault planes are sharp and clear, without proper fault constraints these regularization operators may smooth through rather than preserve these geologic features in the image. To impose explicit constraints on fault planes during LSM, we propose to use convolutional neural networks (CNNs) to detect faults on the migration image first, and then to use the picked fault information as a weighting function built into the regularization scheme during LSM.

Fault picking based on deep learning

Numerous methods have been proposed to detect faults by calculating attributes of seismic reflection continuity such as semblance and coherency (Wu, 2017). These seismic attributes, however, can be sensitive to noise and stratigraphic features. Machine learning is becoming more useful in seismic interpretation, with one of its most successful applications being for fault picking on seismic images. Most recently, some CNN methods have been introduced to detect faults by pixel-wise fault classification (fault or non-fault) with multiple seismic attributes (Wu et al., 2019). Here we follow the work of Wu et al., which considers fault detection as an efficient end-to-end binary image segmentation problem by using CNNs. It generates accurate fault likelihood maps on real datasets by using multiple powerful CNN architectures to obtain superior segmentation results. We use an efficient end-to-end CNN, simplified from U-Net (Ronneberger et al., 2015) and a balanced cross-entropy loss function for optimizing the parameters of the CNN model. Also, to avoid tedious work and obtain a large set of learning data, we use their approach to generate 3D synthetic seismic images and corresponding fault interpretations by randomly choosing a combination of parameters plus artificial noise to train and validate the neural network.

We train our CNN model in two steps. First, we repeat the procedure of Wu et al. by training and validating with 200 and 20 pairs of synthetic seismic and fault images with only random noise added on, respectively. The resulting CNN model cannot distinguish between faults and migration swings when only random noise is added to a field dataset which is heavily contaminated by cross-line migration swings. Since Tensorflow and Keras allow for continued training based on a pre-loaded model, we next added migration swings to each synthetic image. Starting from the previous pretrained CNN model we continue the training process until the training and validation accuracy converges. The CNN model we obtain from this second training step performs better than the pretrained model in distinguishing faults from migration swings, for both synthetic (Figure 1) and real datasets (Figures 2, 4, 5d). As in Wu et al. (2019) the training samples turned out to be sufficient to train a good CNN model for our fault detection needs.

Figure 1. *Fault picking on synthetic validation examples: Inline (top row) and crossline (bottom row) for (a) input image for prediction, (b) fault prediction using pretrained model, (c) final model, and (d) true answers. The final trained model is generally better than the pretrained model in avoiding false picks on migration noise.*

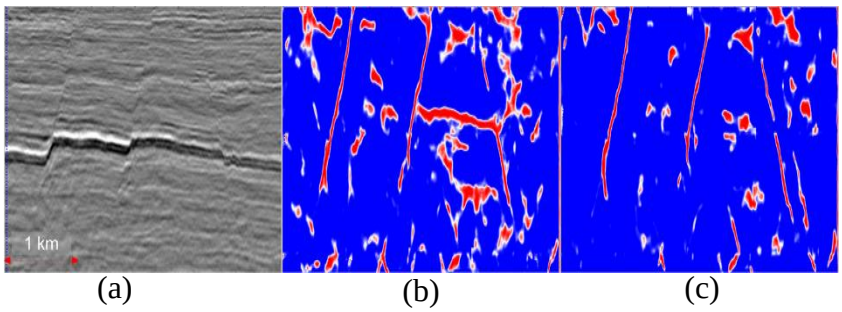

Figure 2. *Fault interpretation on real data migration: (a) input image for prediction, (b) fault likelihood prediction using the pretrained model, and (c) the final model. On real data, the final trained model also performs better than the pretrained model in avoiding false picks on migration noise.*

Least-Squares Migration with structure constraint results

The objective function of regularized LSM can be expressed as:

$$f(\bar{m}) = \min_{\bar{m}} \|\bar{d} - A\bar{m}\|^2 + \lambda \cdot \|D\bar{m}\|_2^2$$

where $f(\bar{m})$ stands for the cost function to be minimized, A is the linearized Born modeling operator which is the exact adjoint of the migration operator and D is a regularization operator. We adopt structure-oriented smoothing with edge-preservation as regularization (Hale, 2009) in LSM to suppress migration artifacts caused by irregular sampling or overfitting to the data noise. The semblance calculation is based on structural tensors and is imposed as a smoothing weight, which allows us to impose fault likelihood as an additional constraint during inversion. In this study, an acoustic one-way wave-equation operator and its adjoint are used.

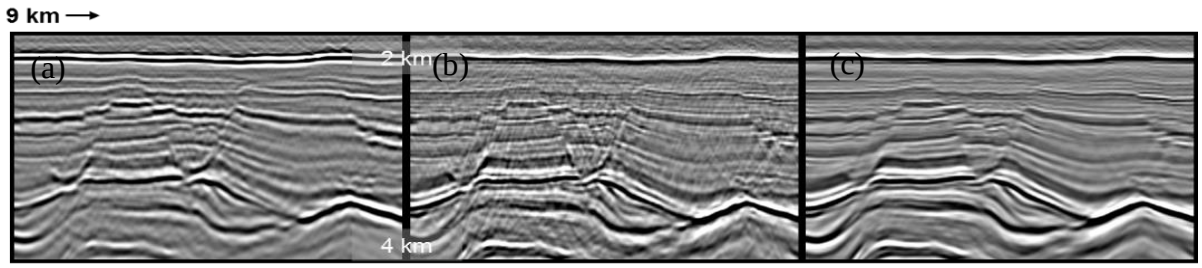

Figure 3. *Inline image for Santos Basin field data examples: (a) conventional migration, (b) LSM at 5th iteration without any regularization, (c) LSM with conventional structure smoothing at 5th iteration.*

We demonstrate our least-squares migration algorithm with a field data example in Santos Basin, offshore Brazil, migrating to 25 Hz on a small volume of the survey. This is a narrow azimuth dataset (NAZ), acquired with 10 cables, 100 m streamer separation and 8 km streamer length. The input data underwent a typical processing flow involving denoise, deghost, demultiple and velocity model building steps. Although this achieves an overall significant improvement over the legacy data, pre-salt and supra-salt images in this area still suffer from uneven illumination, visible migration artifacts, and sub-

optimal resolution. Figure 3b shows LSM without any regularization constraints at iteration 5. Compared to the conventional migration (Figure 3a), LSM shows better events continuity and illumination and higher resolution. However, it also boosts noise content and migration artifacts that are likely caused by overfitting of some events that were present in the input data but could not be correctly modeled by acoustic Born modeling. Figure 3c shows LSM with traditional structural smoothing regularization added during inversion, which generally removes the noise but also sacrifices the spatial resolution on dipping events and fault plane interpretability.

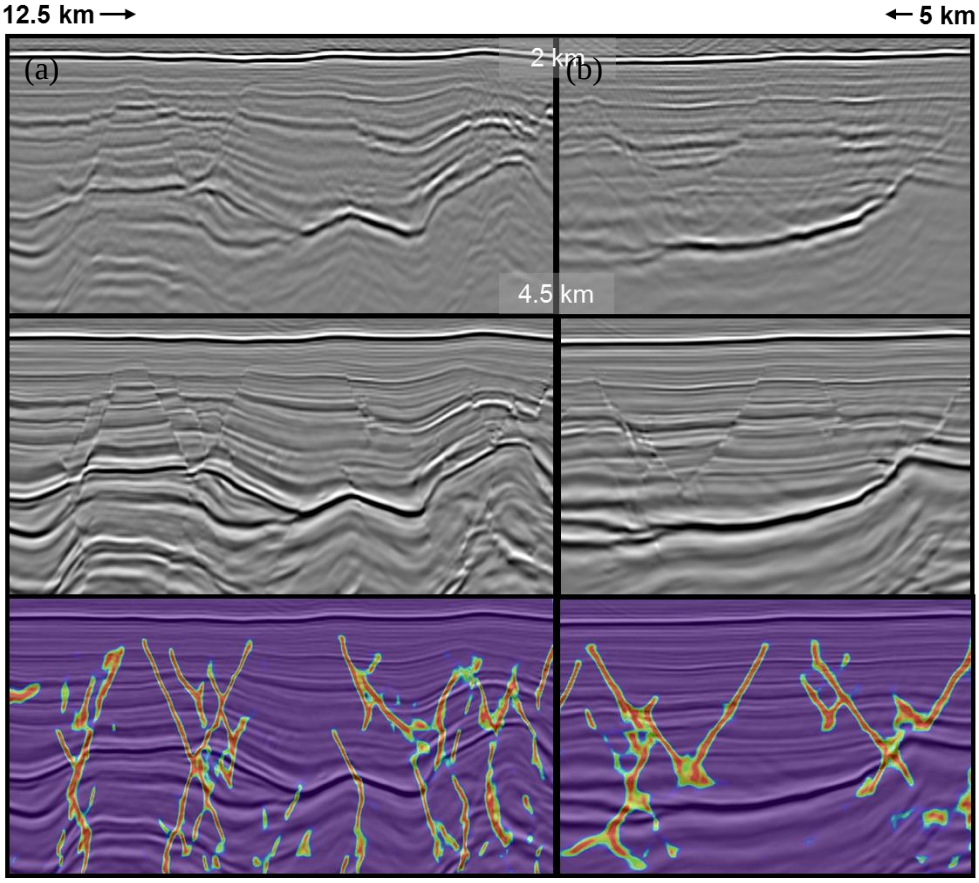

Figure 4. *Santos Basin field data examples: (a) inline image and (b) crossline image. The inline and crossline positions are indicated on Fig. 5a. The top row is the conventional migration to 25Hz; the middle row shows the final structure-constrained LSM image at 5th iteration; the bottom row shows machine-picked fault probability.*

As shown in Figures 4 and 5, our deep learning structure-constrained least-squares technique helps resolve these problems, and the final image is better suited to reservoir characterization. Figure 4 shows the comparison between the final LSM image at iteration 5 and conventional migration in inline and crossline directions. With proper weighting during structure-oriented smoothing, the final result shows all the benefits of conventional LSM without boosting overfitting noise. Compared with conventional regularization, LSM results in higher lateral resolution and clearer, sharper dipping fault planes. Figure 5 shows a depth slice comparison at around 2.8 km in the same volume. It clearly indicates an enhancement in imaging the fault planes and improving spatial resolution, which is quantified by the spectrum comparison in Figure 5c.

Conclusion

Many applications of machine learning in seismic processing have shown that this technique is useful in geological feature characterization, such as fault and salt interpretation. Our work here demonstrates that it is valuable and efficient not only in interpretation but also during image processing itself. The data-domain LSM is an iterative inversion process which needs further constraints to converge to the most geologically sensible solution. We found that combining machine learning constraints and conventional regularization can continue to improve the algorithm's results and bring LSM closer to its full potential. The current trained fault prediction model can make accurate picks even on noisy field seismic data, and the CNN model accuracy can be further improved to help fault interpretation.

With our advanced deep learning structure-constrained LSM algorithm, improved imaging of sedimentary geometries and higher accuracy of fault patterns can be achieved within fewer than 5 iterations for most field data cases. The final least-squares migration images with Santos Basin field dataset also show enhanced fault structure, minimized migration artifacts, significantly increased image resolution and improved illumination. Modern advanced imaging techniques like FWI and LSM are required to run within limited production time for high quality large-scale multi-client projects. With help from machine learning, our highly efficient and automated LSM technique is making this possible.

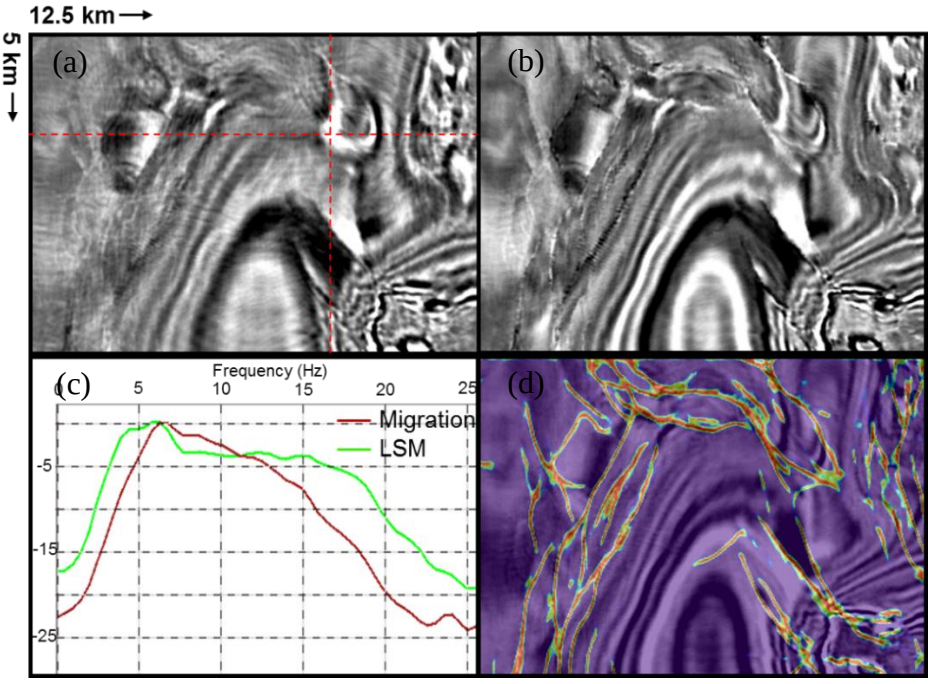

Figure 5. *Depth slice at around 2.8 km of the Santos Basin field data examples: (a) conventional migration image; dashed lines show the location of the inline (Fig.4 a) and crossline (Fig.4b), (b) final structure-constrained LSM image at 5th iteration, (c) whole volume spectrum comparison, and (d) machine-picked fault probability.*

Acknowledgement

The authors would like to thank TGS management for permission to publish this paper. We also thank Yao Zhao for pre-processing the shown real data examples. A special thanks to Guy Hilburn for proofreading this abstract.

References

Hale, D. [2009] Structure-oriented smoothing and semblance: *CWP Report*, 635.

Ronneberger, O., Fischer, P. and Brox, T. [2015] U-net: Convolutional networks for biomedical image segmentation: *International Conference on Medical image computing and computer-assisted intervention*, Springer, 234–241.

Wang, P., Gomes, A., Zhang, Z. and Wang, M. [2016] Least-squares RTM: Reality and possibilities for subsalt imaging. *86th Annual International Meeting*, SEG, Expanded Abstracts, 4204-4209.

Wang, B., Dong, S. and Suh, S. [2013] Practical aspects of least-squares reverse time migration: *75th Conference and Exhibition*, EAGE, Extended Abstracts.

Wu, X. [2017] Directional structure-tensor based coherence to detect seismic faults and channels: *Geophysics*, **82**(2), A13–A17.

Wu, X., Liang, L., Shi, Y. and Fomel S., [2019] FaultSeg3D: Using synthetic data sets to train an end-to-end convolutional neural network for 3D seismic fault segmentation: *Geophysics*, **84**(3): IM35-IM45.